Theory of spacetime impetus

Article *in* Physics Essays · December 2021

DOI: 10.4006/0836-1398-34.4.548

2 authors:

Larry M Silverberg
North Carolina State University
91 PUBLICATIONS **795** CITATIONS

SEE PROFILE

Jeffrey W Eischen
North Carolina State University
46 PUBLICATIONS **1,295** CITATIONS

SEE PROFILE

Theory of spacetime impetus

Larry M. Silverberg[a] and Jeffrey W. Eischen[b]
Department of Mechanical and Aerospace Engineering, North Carolina State University, Campus Box 7910, Raleigh, North Carolina 27695-7910, USA

(Received 9 June 2021; accepted 16 October 2021; published online 22 November 2021)

Abstract: This article introduces the theory of spacetime impetus (SI). The theory unites Newtonian theory (NT) and the theory of general relativity (GR). To develop SI, we reformulated NT in spacetime and replaced the particle primitive in NT with the fragment of energy primitive in field theory. SI replaces Newton's second law $F = ma$ governing the motion of particles, where F, m, and a are, respectively, interaction force, mass, and acceleration, with the change equation $P = k$ governing the motion of fragments of energy, where P and k are, respectively, action force and the curvature of a path in spacetime. To verify SI, we conducted three tests: Test 1 predicted the precession angles of Mercury and Jupiter, test 2 predicted the bending angle of light as it grazes the surface of the sun, and test 3 predicted the radius of the photon sphere. All three tests were in agreement with GR, the third corresponding to strong Riemannian curvature in GR. The equations of motion in SI are in terms of Cartesian coordinates and time and are relatively simple to solve. Undergraduate students in science and engineering and others with similar mathematical skills can validate the results for themselves. © *2021 Physics Essays Publication*.
[http://dx.doi.org/10.4006/0836-1398-34.4.548]

Résumé: Cet article introduit une théorie de l'impetus de l'espace-temps (IET). Cette theorie unifie la Théorie Newtonienne (TN) et la Théorie de la Relativité Générale (TRG) Pour développer cette théorie, nous reformulons la TN dans l'espace-temps et remplaçons la particule primitive décrite par la TN par le fragment d'énergie primitive décrit par la théorie des champs. Dans cette théorie de l'IET, on remplace la seconde loi de Newton $F = ma$ qui régit le mouvement des particules, où F, m, et a sont respectivement une force d'interaction, une masse et une accélération, par l'équation du changement $P = k$ qui gouverne le mouvement de fragments d'énergie, où P et k sont respectivement une force d'action et la courbure d'un trajet dans l'espace-temps. Afin de vérifier cette théorie de l'IET, nous avons effectué trois tests: Le Test 1 a permis de prédire les angles de précession de Mercure et de Jupiter, le test 2 a permis de prédire l'angle de courbure de la lumière lorsqu'elle frôle la surface du Soleil, le test 3 a permis de prédire le rayon d'une sphère de photons. Les résultats des trois tests sont en accord avec la TRG, le troisième correspondant à une forte courbure Riemannienne. Les équations du mouvement dans la théorie de l'IET sont exprimées en fonction de coordonnées Cartésiennes et du temps, et sont assez simples à résoudre. Un étudiant de premier cycle en sciences ou en école d'ingénieur, ou avec des compétences mathématiques similaires, pourra effectuer les calculs de validation soi-même.

Key words: Bending of Light; Black Hole; Fragment of Energy; General Relativity; Impetus; Newtonian Theory; Photon Sphere; Spacetime.

I. INTRODUCTION

Impetus expresses the principle that the change in the state of a primitive results from other primitives, not from itself. In Newtonian theory (NT) and in electromagnetism (EM), the primitives are the particle and the wave. In field theory (FT), the primitive is the fragment of energy.[1] This article introduces a new theory of spacetime impetus (SI) that employs the fragment of energy primitive. The development proceeds as follows. Sections II–IV lay the foundation. Section II shows that the radial form of the fragment of energy leads mathematically to relationships between fragments. The relationships show that impetus is naturally a field concept, not a particle concept. Section III reviews spacetime and focuses on limiting conditions that are natural to spacetime that arise when the speed of a fragment approaches zero at one extreme and the speed of light at the other. Section IV applies these ideas to the two-body problem. Section V develops SI. We show that SI is an axiomatically developed mathematical structure that reformulates NT as a FT. Section VI applies the before mentioned limiting conditions to the fragment of energy. Section VII presents empirical results that validate SI. Specifically, we show, with the limiting conditions, that SI predicts the same precession angles of Mercury and Jupiter, the same bending angle of

[a]lmsilver@ncsu.edu
[b]eischen@ncsu.edu

light, and the same photon sphere radius that the theory of general relativity (GR) predicts. Test 3 is of particular note, because it exposes that one does not need to think of the black hole as a general relativistic phenomenon—associated with the bending of spacetime. Section VIII provides some historical context and conceptual results. Specifically, it compares the classical formulation of impetus in NT with the new formulation in spacetime, explaining how SI advances the classical formulation, and for completeness explains how it answers conceptual questions that were unanswered by NT. Section IX summarizes the article.

II. FRAGMENTS OF ENERGY

In FT, physical analysis deals with the interaction between the different parts of a field and physical synthesis with the recombining of those parts into a whole. Mathematically, the parts and the whole are scalar or vector functions of space and of spacetime. The parts are building blocks for the whole, also called primitives—applicable at different scales of interest. They are not to be confused with elements, which possess a particular structure that applies to a particular scale. One refers to the primitives and to the whole as energy fields or as energy.

This section of the article examines primitives that have a radial form and develops mathematical relationships between them. For simplicity, we shall use light units, for which the speed of light is equal to 1, and for which we denote the nondimensional spatial coordinates of a point by x_1, x_2, and x_3. We start with primitives a and b. They are concentrations of energy, which have a radial form—that is, fragments of energy.[1] The two fragments have source points located at (x_{a1}, x_{a2}, x_{a3}) and (x_{b1}, x_{b2}, x_{b3}), respectively. From their source points, they extend radially outward into space (see Fig. 1). As shown, the fragments have unit vectors $(e_{a1}e_{a2}\ e_{a3})$ and $(e_{b1}e_{b2}\ e_{b3})$ corresponding to the directions of their motion in spacetime, and they have path curvature vectors $(k_{a1}k_{a2}, k_{a3})$ and $(k_{b1}k_{b2}, k_{b3})$ corresponding to the change in direction of their motion in spacetime, but we will not say more about them until Section III; focusing here on spatial considerations alone. We express the fragments mathematically by

$$A_a \triangleq m_a u(r_a), \quad A_b \triangleq m_b u(r_b). \tag{1}$$

In Eq. (1), m_a is the nondimensional mass of fragment a, and $r_a \triangleq \sqrt{(x_1 - x_{a1})^2 + (x_2 - x_{a2})^2 + (x_3 - x_{a3})^2}$ is the nondimensional spatial distance between any point in space and its source point. Likewise, for fragment b, we have m_b and $r_b \triangleq \sqrt{(x_1 - x_{b1})^2 + (x_2 - x_{b2})^2 + (x_3 - x_{b3})^2}$. We shall refer to $u(r_a)$ and $u(r_b)$ as unit fragments. One regards the masses m_a and m_b as the intensities of the fragments. Note that, throughout the article, we employ lower case symbols for geometric quantities and their derivatives and upper case symbols for quantities that depend on mass, too.

At this point, the formulation is general. The unit fragments are merely radial functions, and their radial form is unspecified. Despite the generality, one can already see that interesting relationships arise. For example, one sees that $m_a A_b|_a = m_b A_a|_b$ because $r_a|_b = r_b|_a$. (The notation $()|_a$ means evaluated at the source point of fragment a.) Table I lists more relationships.

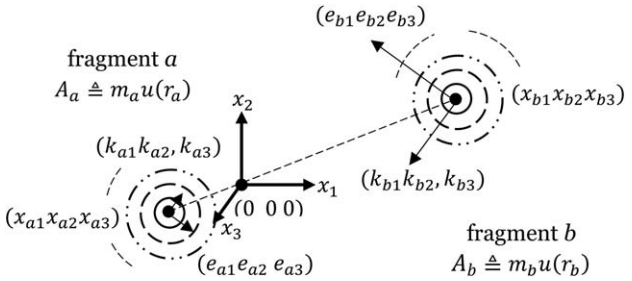

FIG. 1. A two-body system of fragments.

TABLE I. Relationships between fragments of energy.

Radial functions	
$r_a\|_b = r_b\|_a \triangleq r_{ab}$	
$\frac{\partial r_a}{\partial x_s} = \frac{x_s - x_{as}}{r_a}$	$\frac{\partial r_a}{\partial x_{as}} = -\frac{x_s - x_{as}}{r_a}$
$\frac{\partial r_a}{\partial x_s} = -\frac{\partial r_a}{\partial x_{as}}$	$\left.\frac{\partial r_b}{\partial x_s}\right\|_a = -\left.\frac{\partial r_a}{\partial x_s}\right\|_b$
Unit fragments of energy	
$u(r_a)\|_b = u(r_b)\|_a$	$\left.\frac{du(r_a)}{dr_a}\right\|_b = \left.\frac{du(r_b)}{dr_b}\right\|_a$
Fragments of energy	
$m_a A_b\|_a = m_b A_a\|_b$	
$\frac{\partial A_a}{\partial x_s} = m_a \frac{du(r_a)}{dr_a}\frac{\partial r_a}{\partial x_s}$	$\frac{\partial A_a}{\partial x_{as}} = m_a \frac{du(r_a)}{dr_a}\frac{\partial r_a}{\partial x_{as}}$
$\frac{\partial A_a}{\partial x_s} = -\frac{\partial A_a}{\partial x_{as}}$	

The relationships between the fragments of energy in Table I motivate the naming of quantities in Table II with the term action and interaction, where we appropriated these terms from the philosophy of science community.[c]) Table II defines the named quantities and shows additional relationships deduced from Table I.

Line 1 in Table II defines P_{as} and P_{bs} as action forces that act on fragments a and b, respectively, and deduces relationships between them in line 4. In line 5, we refer to F_{as} and F_{bs} as interaction forces and deduce the relationships between them in line 6. Line 7 defines Q_{at} and Q_{bt} as action moments, respectively, and deduces relationships between them in line 8. Line 9 defines M_{at} and M_{bt} as interaction moments and deduces relationships between them in line 10. As shown, one takes the moments about an arbitrary spatial point (x_{01}, x_{02}, x_{03}), and the triad (r, s, t) is a right-handed set of distinct indices.

[c])Action-based theories of perception (2015) https://plato.stanford.edu/entries/action-perception/

TABLE II. Action and interaction.

	Action forces	
1	$P_{as} \triangleq \left.\frac{\partial A_b}{\partial x_s}\right\|_a = G_a(x_{bs} - x_{as}),$	$P_{bs} \triangleq \left.\frac{\partial A_a}{\partial x_s}\right\|_b = -G_b(x_{bs} - x_{as})$
2	$G_a \triangleq \left.\frac{du(r_b)}{dr_b}\right\|_a \frac{m_b}{r_{ab}}$	$G_b \triangleq \left.\frac{du(r_a)}{dr_a}\right\|_b \frac{m_a}{r_{ab}}$
3	$m_a G_a + m_b G_b = 0$	
4	$m_a P_{as} + m_b P_{bs} = 0$	
	Interaction forces	
5	$F_{as} \triangleq m_a P_{as}$	$F_{bs} \triangleq m_b P_{bs}$
6	$F_{as} + F_{bs} = 0$	
	Action moments	
7	$Q_{at} \triangleq (x_{ar} - x_{0r})P_{as} - (x_{as} - x_{0s})P_{ar} = 0$	$Q_{bt} \triangleq (x_{br} - x_{0r})P_{bs} - (x_{bs} - x_{0s})P_{br} = 0$
8	$m_a Q_{at} + m_b Q_{bt} = 0$	
	Interaction moments	
9	$M_{at} \triangleq m_a Q_{at}$	$M_{bt} \triangleq m_b Q_{bt}$
10	$M_{at} + M_{bt} = 0$	

From Table II, we see in line 1 that forces act along the line through the source points of the fragments, in line 6 that interaction forces are equal in magnitude and opposite in direction, and in line 10 that interaction moments are equal in magnitude and opposite in direction, too. One skilled in the art understands that one can extend these relationships from the single pair of fragments of energy given in Eq. (1) to a discrete system of n fragments of energy, and further to a distributed system of fragments (see Appendix B). Moreover, the existence of these field relationships, which rest solely on Eq. (1) without specifying the forms of the radial functions, strongly suggests that impetus is a field concept, not a particle concept as classically believed, and that one might be able to reformulate the classical conception of impetus so that it becomes fully consistent with FT.

III. SPACETIME

In FT and in SI, in particular, the field acts over a spacetime domain, not a spatial domain. For simplicity, we shall continue to use light units. The coordinates of a point in the domain are t, x_1, x_2, and x_3, where t is the nondimensional time and the others, as before, are nondimensional spatial coordinates. The point is along an arbitrary spacetime path. In this article, it will correspond to the source point of a fragment. The square of the spacetime metric ds associated with the spacetime path of the point is

$$ds^2 \triangleq dt^2 - dx_1^2 - dx_2^2 - dx_3^2. \tag{2}$$

Appendix A gives the spacetime operations, based on Eq. (2), for the scalar product and for perpendiculars. In Eq. (2), dt, dx_1, dx_2, and dx_3 are coordinate increments. Dividing the metric by the time increment dt and the coordinates by the path increment ds

$$\begin{aligned}
\left(\frac{ds}{dt}\right)^2 &= 1 - \left(\frac{dx_1}{dt}\right)^2 - \left(\frac{dx_2}{dt}\right)^2 - \left(\frac{dx_3}{dt}\right)^2 \\
&= 1 - v_1^2 - v_2^2 - v_3^2 = 1 - v^2, v_r = \frac{dx_r}{dt} \\
e_r &\triangleq \frac{dx_r}{ds} = \frac{dt}{ds} v_r = \beta v_r, \quad (r = 1, 2, 3) \\
\beta &\triangleq e_0 \triangleq \frac{dt}{ds} = \frac{1}{(1 - v^2)^{1/2}}
\end{aligned} \tag{3}$$

In Eq. (3), e_r ($r = 0$, 1, 2, and 3) are the components of the unit tangent to the spacetime path (see Fig. 1). Above, we expressed them in terms of their velocity components v_1, v_2, and v_3, and their magnitude v. Next, let us calculate

$$\frac{d\beta}{ds} = \frac{dt}{ds}\frac{d\beta}{dt} = \frac{1}{(1 - v^2)^{1/2}} \frac{v_s a_s}{(1 - v^2)^{3/2}} = \frac{v_s a_s}{(1 - v^2)^2},$$
$$a_r = \frac{dv_r}{dt},$$

where a_r ($r = 1$, 2, and 3) are acceleration components. (We sum repeated indices from 1 to 3.) From this expression and Eq. (3), we define the path curvature components by

$$\begin{aligned}
k_r &\triangleq \frac{de_r}{ds} = \frac{d}{ds}(\beta v_r) = \frac{d\beta}{ds} v_r + \beta \frac{dv_r}{ds} = \frac{d\beta}{ds} v_r + \beta^2 a_r \\
&= \frac{v_s a_s}{(1 - v^2)^2} v_r + \beta^2 a_r \qquad (r = 1, 2, 3) \\
&= \left[\frac{1}{(1 - v^2)^2} v_r v_s + \frac{1}{1 - v^2} \delta_{rs}\right] a_s
\end{aligned} \tag{4}$$

where δ_{rs} is the Kronecker-delta function.[2] The term path curvature for the components in Eq. (4) comes from the

mathematics community[1] and is not to be confused with the term Riemannian curvature used in GR. The term path curvature used here is the path derivative of the unit vector tangent to the spacetime path, which is perpendicular to the spacetime path. It corresponds to the level at which a spacetime path bends, whereas Riemannian curvature corresponds to the curvature of spacetime *itself*. When reading further, you will find that the curvature of a path in spacetime supplants the acceleration of a path in space that one employs in classical physics. Equation (4) establishes the important connection between spacetime path curvature and spatial acceleration.

A. Limiting behaviors

Below, we focus on the limiting behaviors of speed approaching 0 and 1. We start by rewriting Eq. (4) as

$$k_r = A_{rs}a_s, A_{rs} \triangleq \frac{1}{(1-v^2)^2} v_r v_s + \frac{1}{1-v^2}\delta_{rs} \quad (r,s=1,2,3). \tag{5}$$

In Eq. (5), A_{rs} governs the transformation from acceleration to path curvature. It also follows that the inverse transformation from path curvature to acceleration and its solution are

$$a_r = B_{rs}k_s, \quad B_{rs} \triangleq (1-v^2)(-v_r v_s + \delta_{rs}) \quad (r,s=1,2,3). \tag{6}$$

Figure 2 gives a geometric interpretation of Eq. (6). As shown, the acceleration becomes perpendicular to the velocity as v approaches 1. To see this more completely, one can decompose these transformations by inspecting their eigensolutions. The transformation A_{rs} is real and symmetric, so its eigensolution is real. The orthonormal eigensolution of the associated eigenvalue problem $A_{rs}\phi_s^{(r)} = \lambda_s \phi_s^{(r)}$, $(r=1,2,3)$, is

$$\lambda_1 = \frac{1}{(1-v^2)^2}, \quad \phi_s^{(1)} = \frac{1}{v}\begin{pmatrix} v_1 \\ v_2 \\ v_3 \end{pmatrix}, \quad v^2 = v_1^2 + v_2^2 + v_3^2,$$

$$\lambda_2 = \frac{1}{1-v^2}, \quad \phi_s^{(2)} = \frac{1}{v_{12}}\begin{pmatrix} -v_2 \\ v_1 \\ 0 \end{pmatrix}, \quad v_{12}^2 = v_1^2 + v_2^2,$$

$$\lambda_3 = \frac{1}{1-v^2}, \quad \phi_s^{(3)} = \frac{1}{vv_{12}}\begin{pmatrix} v_1 v_3 \\ v_2 v_3 \\ -v_{12}^2 \end{pmatrix}. \tag{7}$$

We see that the first eigenvector $\phi_s^{(1)}$ aligns with the velocity components and that the second and third eigenvectors, $\phi_s^{(1)}$ and $\phi_s^{(2)}$, which have repeated eigenvalues, are

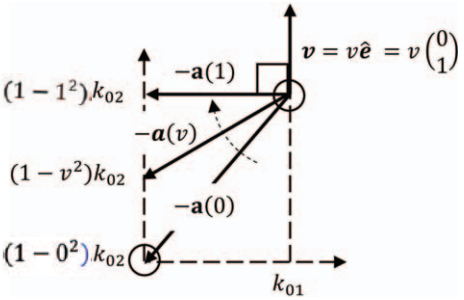

FIG. 2. $\mathbf{a}(v) = \begin{pmatrix} k_{01} \\ (1-v^2)k_{02} \end{pmatrix}$ in the x_1-x_2 plane, holding constant $\mathbf{k}_0 = \begin{pmatrix} k_{01} \\ k_{02} \end{pmatrix} \triangleq (1-v^2)\begin{pmatrix} k_1 \\ k_2 \end{pmatrix}$ and $\hat{\mathbf{e}} \triangleq \begin{pmatrix} e_1 \\ e_2 \end{pmatrix}$.

perpendicular to the velocity components. Next, expand the acceleration components and the path curvature components in terms of the eigensolution to get

$$\mathbf{a} \triangleq \begin{pmatrix} a_1 \\ a_2 \\ a_3 \end{pmatrix} = \phi_1\mu_1 + \phi_2\mu_2 + \phi_3\mu_3 = \frac{1}{v}\begin{pmatrix} v_1 \\ v_2 \\ v_3 \end{pmatrix}\mu_1 + \frac{1}{v_{12}}\begin{pmatrix} -v_2 \\ v_1 \\ 0 \end{pmatrix}\mu_2 + \frac{1}{vv_{12}}\begin{pmatrix} v_1 v_3 \\ v_2 v_3 \\ -v_{12}^2 \end{pmatrix}\mu_3,$$

$$\mathbf{k} \triangleq \begin{pmatrix} k_1 \\ k_2 \\ k_3 \end{pmatrix} = \lambda_1\phi_1\mu_1 + \lambda_2\phi_2\mu_2 + \lambda_3\phi_3\mu_3 = \frac{\lambda_1}{v}\begin{pmatrix} v_1 \\ v_2 \\ v_3 \end{pmatrix}\mu_1 + \frac{\lambda_2}{v_{12}}\begin{pmatrix} -v_2 \\ v_1 \\ 0 \end{pmatrix}\mu_2 + \frac{\lambda_3}{vv_{12}}\begin{pmatrix} v_1 v_3 \\ v_2 v_3 \\ -v_{12}^2 \end{pmatrix}\mu_3, \tag{8}$$

where

$$\mu_1 = a_s\phi_s^{(1)} = \frac{1}{v}(a_1v_1 + a_2v_2 + a_3v_3),$$
$$\mu_2 = a_s\phi_s^{(2)} = \frac{1}{v_{12}}(-a_1v_2 + a_2v_1), \tag{9}$$
$$\mu_3 = a_s\phi_s^{(3)} = \frac{1}{vv_{12}}\left(a_1v_1v_3 + a_2v_2v_3 - a_3v_{12}^2\right).$$

Let us now examine the limiting behaviors at the two extremes of v approaching 0 and 1, wherein we assume that v_r and a_r are finite. First, when v approaches 0, it follows from Eqs. (3) and (4) that e_r converges to v_r and that k_r converges to a_r. Indeed, spacetime geometry converges to ordinary geometry when v approaches 0, as expected. Next, consider Eqs. (3) and (4) when v approaches 1. At this extreme, e_r and k_r become unbounded because of the $1-v^2$ terms in the denominators. To examine more closely this limiting behavior, consider Eqs. (8) and (9). First, notice that the coefficients μ_1, μ_2, and μ_3 in Eq. (9) must be finite, assuming that the acceleration components

are finite. Next, consider the possibility that k_r is on the order of $1/(1-v^2)$, written as $k_r \sim 1/(1-v^2)$. When this is the case, it follows from Eq. (8) that $\mu_1 \sim (1-v^2)$. The acceleration components become perpendicular to the velocity components, and the speed v becomes a terminal speed as v approaches 1. Under this *curvature condition*, the spacetime path can still bend because the components of acceleration are perpendicular to the components of velocity. We will impose this curvature condition later, when developing a specific form of the unit fragment of energy that conforms to physical behavior at the speed of light.

IV. THE TWO-BODY PROBLEM

Assume that one measures time and spatial quantities in an inertial frame, and that one does *not* measure them in any other frames. When employing the inertial frame, the time increments of the moving centers of the two previously considered fragments are the same. Table III shows for the two-body problem how their treatments differ when employing ordinary geometry and spacetime geometry. As shown, Table III indicates the differences in the treatments of increments, time variables, differentiation, and integration. Table IV describes the two-body problem when employing spacetime geometry and Table V when employing ordinary geometry. For those less familiar with spacetime geometry, an unusual and telling difference between the treatments rests in the expressions for the mass center c. For example, compare the spatial components of the mass center and the velocity components of the mass center in ordinary geometry (lines 1 and 2 in Table V) with the corresponding components in spacetime geometry (lines 1 and 2 in Table IV)

$$\begin{aligned} x'_{cs} &\triangleq \frac{1}{m_a+m_b}\left(m_a x'_{as} + m_b x'_{bs}\right), \\ v'_{cs} &\triangleq \frac{1}{m_a+m_b}\left(m_a v'_{as} + m_b v'_{bs}\right), \\ e'_{cs} &\triangleq \frac{1}{m_a+m_b}\left(m_a e'_{as} + m_b e'_{bs}\right). \end{aligned} \tag{10}$$

As shown, the spatial components of the mass center in ordinary geometry are the same as in spacetime geometry, but the spatial components of the velocity components of the mass center and of the unit vector components in spacetime geometry differ. When employing ordinary geometry, one differentiates in time the spatial components of the mass center to obtain the velocity components. The time increment for both fragments is the same. However, when employing

TABLE III. The time variable in ordinary geometry and the time variable in spacetime geometry.

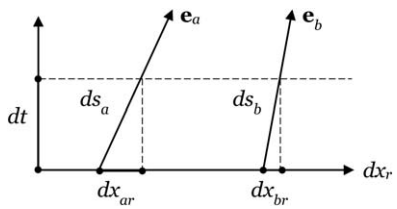

	Ordinary geometry	**Spacetime geometry**
Increment	The time increment dt is the same for a and for b	The path increments dsa and dsb are different for a and for b
Time variable	Independent variable	Geometric coordinate, satisfies metric condition
Differentiation	$\frac{dx_{ar}}{dt}, \frac{dx_{br}}{dt}$	$\frac{dx_{ar}}{ds_a} = \frac{dt}{ds_a}\frac{dx_{ar}}{dt}, \frac{dx_{br}}{ds_b} = \frac{dt}{ds_b}\frac{dx_{br}}{dt}$
Integration	Integrate over time	Integrate over spacetime path

TABLE IV. The two-body problem in spacetime geometry.

	Spacetime geometry ($s = 1$, 2, and 3)			
1	$x'_{cs} \triangleq \frac{1}{m_a+m_b}(m_a x'_{as}+m_b x'_{bs})$		$x_{abs} \triangleq x'_{bs} - x'_{as}$	
2	$e'_{cs} \triangleq \frac{1}{m_a+m_b}(m_a e'_{as}+m_b e'_{bs})$		$e_{abs} \triangleq e'_{bs} - e'_{as}$	
3	$k'_{cs} \triangleq \frac{1}{m_a+m_b}(m_a k'_{as}+m_b k'_{bs})$		$k_{abs} \triangleq k'_{bs} - k'_{as}$	
		Point a	Point b	Point c
4	$x_s \triangleq x'_s - x'_{cs}$	$x_{as} = -\frac{m_b}{m_a+m_b}x_{abs}$	$x_{bs} = \frac{m_a}{m_a+m_b}x_{abs}$	$x_{cs} = x'_{cs} - x'_{cs} = 0$
5	$e_s \triangleq e'_s - e'_{cs}$	$e_{as} = -\frac{m_b}{m_a+m_b}e_{abs}$	$e_{bs} = \frac{m_a}{m_a+m_b}e_{abs}$	$e_{cs} = e'_{cs} - e'_{cs} = 0$
6	$k_s \triangleq k'_s - k'_{cs}$	$k_{as} = -\frac{m_b}{m_a+m_b}k_{abs}$	$k_{bs} = \frac{m_a}{m_a+m_b}k_{abs}$	$k_{cs} = k'_{cs} - k'_{cs} = 0$

TABLE V. The two-body problem in ordinary geometry.

	Ordinary geometry ($s=1$, 2, and 3)			
1	$x'_{cs} \triangleq \frac{1}{m_a+m_b}(m_a x'_{as}+m_b x'_{bs})$		$x_{abs} \triangleq x'_{bs} - x'_{as}$	
2	$v'_{cs} \triangleq \frac{1}{m_a+m_b}(m_a v'_{as}+m_b v'_{bs})$		$v_{abs} \triangleq v'_{bs} - v'_{as}$	
3	$a'_{cs} \triangleq \frac{1}{m_a+m_b}(m_a a'_{as}+m_b a'_{bs})$		$a_{abs} \triangleq a'_{bs} - a'_{as}$	
		Point a	Point b	Point c
4	$x_s \triangleq x'_s - x'_{cs}$	$x_{as} = -\frac{m_b}{m_a+m_b}x_{abs}$	$x_{bs} = \frac{m_a}{m_a+m_b}x_{abs}$	$x_{cs} = x'_{cs} - x'_{cs} = 0$
5	$v_s \triangleq v'_s - v'_{cs}$	$v_{as} = -\frac{m_b}{m_a+m_b}v_{abs}$	$v_{bs} = \frac{m_a}{m_a+m_b}v_{abs}$	$v_{cs} = v'_{cs} - v'_{cs} = 0$
6	$a_s \triangleq a'_s - a'_{cs}$	$a_{as} = -\frac{m_b}{m_a+m_b}a_{abs}$	$a_{bs} = \frac{m_a}{m_a+m_b}a_{abs}$	$a_{cs} = a'_{cs} - a'_{cs} = 0$

spacetime geometry, the differentiations are along spacetime path increments and they differ, even though their time increments are the same. To see this more clearly in the expressions above, let us write explicitly the differentiations

$$\frac{dx'_{cs}}{dt} \triangleq \frac{1}{m_a+m_b}\left(m_a\frac{dx'_{as}}{dt}+m_b\frac{dx'_{bs}}{dt}\right),$$
$$\frac{dx'_{cs}}{ds_c} \triangleq \frac{1}{m_a+m_b}\left(m_a\frac{dx'_{as}}{ds_a}+m_b\frac{dx'_{bs}}{ds_b}\right). \tag{11}$$

In spacetime, the path differentiation of the mass center (the left side) and the sum of the path differentiations of the individual fragments (the right side) are different. The concepts of mass and of mass center lose their meaning as the speed of a fragment approaches the speed of light. In spacetime geometry, the concept of mass center possesses a *mass center speed limitation*.[3]

We began in lines 1–3 of Tables IV and V with primed coordinates, upon which we imposed no prior assumptions, and defined the relative positions of the mass centers of the fragments and of their first two derivatives. In lines 4–6, we set up translated coordinates relative to the mass center. These are the coordinates of the inertial frame. Notice that the translation does not rotate the original frame of reference. This is important to recognize because, in physical problems, one obtains different results with frames of reference that are rotating differently relative to the fixed stars.

Finally, let us define in Table VI the linear momentum of each fragment and of the two-body system, the angular rate of each fragment, and the angular momentum of each fragment and of the two-body system.

The angular rate components h_{at} and h_{bt} in line 3 are the "rotational" counterparts to the unit vector components e_{ar} and e_{br} in line 5 of Table IV. One says that the angular rate components and the angular momentum components are *about* the spatial point (x_{01}, x_{02}, x_{03}).

V. THEORY OF SI

The field concept, as it applies to fragments of energy described in Section II, the limiting behavior of spacetime described in Section III, and the two-body problem in Section IV, provide a mathematical foundation for the development of SI. In words, the spacetime concept of impetus equates the change in the spacetime path that one fragment of energy undergoes to the change that it experiences from other fragments of energy. In the two fragments under consideration, $dA_a|_b$ represents mathematically the incremental change that fragment b "experiences" due to fragment a, and $dA_b|_a$ represents mathematically the incremental change that fragment a experiences due to fragment b. Invoking this principle in each "coordinate direction"

$$P_{as} = k_{as}, \quad P_{bs} = k_{bs}, \quad (s=1,2,3). \tag{12}$$

We shall refer to Eq. (12) as the *spacetime change equations*. Also, let us now understand better what we mean by "experiencing" a change and by "coordinate direction". To that end, we recognize that each fragment is a function of the spacetime coordinates of any point in the inertial frame as well as the spacetime coordinates in the inertial frame of its source point. From the bottom line in Table I, the incremental changes of fragments a and b are

$$dA_a = \frac{\partial A_a}{\partial x_s}dx_s + \frac{\partial A_a}{\partial x_{as}}dx_{as} = \frac{\partial A_a}{\partial x_s}(dx_s - dx_{as}),$$
$$dA_b = \frac{\partial A_b}{\partial x_s}dx_s + \frac{\partial A_b}{\partial x_{bs}}dx_{bs} = \frac{\partial A_b}{\partial x_s}(dx_s - dx_{bs}), \tag{13}$$

TABLE VI. Linear momentum, angular rate, and angular momentum.

	Linear momentum
1	$L_{ar} \triangleq m_a e_{ar}$, $L_{br} \triangleq m_b e_{br}$
2	$L_r \triangleq L_{ar} + L_{br}$
	Angular rate
3	$h_{at} \triangleq (x_{ar} - x_{0r})e_{as} - (x_{as} - x_{0s})e_{ar}$, $h_{bt} \triangleq (x_{br} - x_{0r})e_{bs} - (x_{bs} - x_{0s})e_{br}$
	Angular momentum
4	$H_{at} \triangleq m_a h_{at}$, $H_{bt} \triangleq m_b h_{bt}$
5	$H_t \triangleq H_{at} + H_{bt}$

where, again, we sum over s from 1 to 3. From Eq. (13), line 1 in Table II, and Eq. (12)

$$\begin{aligned} dA_a|_b &= P_{bs}(dx_{bs} - dx_{as}) = k_{bs}(dx_{bs} - dx_{as}), \\ dA_b|_a &= P_{as}(dx_{as} - dx_{bs}) = k_{as}(dx_{as} - dx_{bs}). \end{aligned} \tag{14}$$

First, consider that we mean for an experience of an incremental change by one fragment to refer to an evaluation of an incremental change of another fragment of energy at the source point of the one fragment of energy. Furthermore, the incremental change is a sum across spatial coordinates; we mean for coordinate directions to refer to the terms in the sum in Eq. (14). Let us now examine Eq. (14) more closely to appreciate better the implied relationships expressed in the change equations. First, notice if $k_{bs} = 0$ then $dA_a|_b = 0$. In words, fragment b does not experience an incremental change $dA_a|_b$ from fragment a when fragment b is moving along a straight spacetime path, which corresponds to motion that is constant in speed and direction. Likewise, fragment a does not experience an incremental change $dA_b|_a$ from fragment b when fragment a is moving along a straight spacetime path. Next, consider the possibility that $dx_{bs} - dx_{as} = 0$. When this occurs, the incremental change $dA_a|_b$ is zero, too. In words, fragment b does not experience a change $dA_a|_b$ when its path increment relative to fragment a is equal to zero. This occurs when the forces P_{as} and P_{bs} between the fragments prevent a relative change from occurring. Similarly, fragment a does not experience a change $dA_b|_a$ when its path increment relative to fragment b is equal to zero. Finally, consider the converse. When $dA_a|_b$ is equal to zero, either $k_{bs} = 0$ or $dx_{bs} - dx_{as} = 0$. In the first case, $P_{bs} = 0$, and in the second case, a force acts on fragment b to maintain the condition that there is no relative change in the path increment. When $dA_b|_a$ is equal to zero, we get the corresponding result. In short, one fragment does not experience an incremental change from the other fragment when and only when its *absolute* path curvature is zero or when its path increment *relative* to the other is zero.

Pertaining to linear momentum and angular momentum about a stationary point ($e_{0r} = 0, r = 1, 2, 3$), we obtain the following from the change equations, Table II and Table VI:

$$\begin{aligned} \frac{dL_r}{ds} &\triangleq \frac{dL_{ar}}{ds_a} + \frac{dL_{br}}{ds_b} = m_a k_{ar} + m_b k_{br} = m_a P_{ar} + m_b P_{br} = 0 \\ \frac{dH_t}{ds} &\triangleq \frac{dH_{at}}{ds_a} + \frac{dH_{bt}}{ds_b} \\ &= m_a\big((x_{ar} - x_{0r})k_{as} - (x_{as} - x_{0s})k_{ar}\big) \\ &\quad + m_b\big((x_{br} - x_{0r})k_{bs} - (x_{bs} - x_{0s})k_{br}\big) \\ &= m_a\big((x_{ar} - x_{0r})P_{as} - (x_{as} - x_{0s})P_{ar}\big) \\ &\quad + m_b\big((x_{br} - x_{0r})P_{bs} - (x_{bs} - x_{0s})P_{br}\big) = 0, \end{aligned}$$

that is,

$$\begin{aligned} \frac{dL_r}{ds} &= 0, \\ \frac{dH_t}{ds} &= 0. \end{aligned} \tag{15}$$

In words, Eq. (15) expresses that the linear momentum of the two-body system and the angular momentum of the two-body problem about a stationary point are invariants (see Appendix B for the extension of these results to n-body systems).

Per these developments, SI sets up a mathematical structure for the interaction between fragments of energy in spacetime. It began with Eq. (1), from which we deduced the field results given in Table I and Table II. Next, it employed the spacetime framework set up in Eq. (2), from which we obtained mathematical expressions for e_r and k_r in Eqs. (3) and (4), and the spacetime geometry in Table IV. Then, Eq. (12) expressed mathematically a new interpretation of impetus as spacetime change equations. From this mathematical structure, we defined action forces and moments, interaction force and moments, linear momentum, angular momentum, and showed in Eq. (15) that the linear momentum and angular momentum defined in Table VI are invariants. Finally, again, we point out amazingly that the mathematical structure on which SI rests, leaves the radial dependence of the unit fragments unspecified.

VI. LIMITING CONDITION AT THE SPEED OF LIGHT

Next, we will develop a specific expression for a fragment of energy that conforms to physical behavior at the speed of light. A simple version of that expression was first introduced in Ref. 1, where it was shown to result in predicting the same precession of Mercury as GR predicts, and in predicting the same bending of light as it grazes the sun as GR predicts. That work considered both ordinary geometry and spacetime geometry and showed, when employing that fragment in spacetime, that the corresponding predictions agree with GR (see Tables IV and VI in Ref. 1). In that work, we applied the fragment to one-body problems. We had not yet examined two-body spacetime effects, and we had not thoroughly justified the use of the fragment. Indeed, in Ref. 1, we left open the question whether there was a logical basis for the fragment that is independent of GR. In this section, we answer that question in the affirmative by developing the fragment without invoking GR. Then, in Section VII, we will test the resulting behavior on benchmark two-body problems.

The reasoning in SI that leads to a specific fragment that conforms with light behavior begins with the rationale behind unit fragments of energy of the form

$$u(r_a) \triangleq -\frac{1}{r_a}, \quad u(r_b) \triangleq -\frac{1}{r_b}. \tag{16}$$

As proven in Appendix D of Ref. 1, the form given in Eq. (16) is unique up to a multiplicative constant because the radial power of minus one is the only power for which the stationary fragment satisfies vector continuity (colloquially, it flows[d]). When employing this specific form, one obtains precisely the gravitational potential of a stationary body in NT modeled as a point mass and its corresponding

[d]R. Puyana (2021), "Our Flowing Universe," (video) https://www.youtube.com/watch?v=0cBqtaGdUnI

gravitational force. Next, we consider the case of a moving fragment with a particular interest in motion that approaches the speed of light. From the mathematics of spacetime, we now understand that the interest lies in satisfying the curvature condition, that is, in path curvature converging to the order of the reciprocal of $1-v^2$ ($k_r \sim 1/(1-v^2)$) when v approaches 1. Therefore, we seek fragments of energy of the form

$$u(r_a) \triangleq -\frac{1}{r_a} f(r_a), \quad u(r_b) \triangleq -\frac{1}{r_b} f(r_b), \tag{17}$$

in which $f(r)$ is a function that has the limiting properties

$$\begin{aligned} f(r) &= 1 && \text{as } v \text{ approaches } 0, \\ f(r) &\sim \frac{1}{1-v^2} && \text{as } v \text{ approaches } 1. \end{aligned} \tag{18}$$

Note that v in Eq. (18) can correspond to v_a, v_b, or to the speed v in the one-body problem. In Eq. (18), the intent is for the gravitational form in NT to continue to satisfy vector continuity when $v=0$, and for the correct limiting properties to be satisfied as v approaches 1.

The immediate goal here is to find a fragment that is a radial function without it containing an explicit function of the speed v. Of course, if such a radial form exists, it follows that there must be some relationship between the distance r and the speed v that one can use to eliminate the speed v in Eq. (18). Such invariants as linear momentum, angular momentum, and energy are obvious candidates. Furthermore, we sought a reference case that would expose that radially dependent relationship and found it when examining angular momentum under circular motion. Under circular motion, the total angular momentum is $H = H_{a3} + H_{b3} = r_a m_a e_{a\theta} + r_b m_b e_{b\theta} = r_{ab}\mu e_\theta$, in which $e_\theta = \frac{v}{\sqrt{1-v^2}}$ and $\mu = \frac{m_a m_b}{m_a+m_b}$. The radially dependent dimensionless relationship is

$$\frac{1}{1-v^2} = 1 + \left(\frac{H}{\mu}\right)^2 \frac{1}{r_{ab}^2}.$$

From Eq. (17), the specified radial forms of the unit fragments of energy that satisfy the desired limiting conditions are the fields

$$\begin{aligned} u(r_a) &\triangleq -\frac{1}{r_a}\left(1 + \left(\frac{H}{\mu}\right)^2 \frac{1}{r_a^2}\right), \\ u(r_b) &\triangleq -\frac{1}{r_b}\left(1 + \left(\frac{H}{\mu}\right)^2 \frac{1}{r_b^2}\right). \end{aligned} \tag{19}$$

Equation (19) expresses the sought after specific forms of the two fragments.

As one would expect, the specific fragment developed above does not predict the behavior that would result from an *anisotropic* source, such as from a spinning source. That behavior would require a different fragment—one that is determined by imposing different limiting conditions. However, regardless of the type of source, the process that one follows to determine the form of a fragment of energy should be the same as the one followed above. One first expresses a limiting condition in terms of a speed v, then one identifies a reference case that matches the desired behavior, and finally one determines the desired form of the fragment. Finally, note that the process that one follows in SI of determining a fragment of energy for a particular type of source is analogous to the process that one follows in GR of determining the elements g_{rs} of a metric tensor for a particular type of source. In both approaches, one imposes limiting conditions that correspond to a reference case(s) that produces a desired behavior. The major difference is that the goal in SI is to correctly bend light whereas the goal in GR is to correctly bend spacetime itself.

Tables VII gives the governing equations of motion for the two-body problems. Notice in Table VII that we expressed the acceleration components in nonexpanded and expanded forms. The expanded form distinguishes between powers of $1-v^2$ to highlight which terms are present when $v=0$, when $v=1$, and in between. As shown, we expressed the acceleration components in the expanded form as the sum of three terms surrounded by braces $\{\}$. The direction of the first term is along the line between the two fragments. The directions of the second and third terms are perpendicular to the motion of the fragment. When $v=0$, the first term

TABLE VII. Governing equations for the two-body problems in light units.

Acceleration components of fragment a

$$\begin{pmatrix} a_{a1} \\ a_{a2} \end{pmatrix} = (1-v_a^2)\begin{bmatrix} 1-v_{a1}^2 & -v_{a1}v_{a2} \\ -v_{a1}v_{a2} & 1-v_{a2}^2 \end{bmatrix}\begin{pmatrix} k_{a1} \\ k_{a2} \end{pmatrix}$$

$$\begin{pmatrix} k_{a1} \\ k_{a2} \end{pmatrix} = \begin{pmatrix} P_{a1} \\ P_{a2} \end{pmatrix} = Gm_b\left(1 + 3\left(\frac{H}{\mu}\right)^2 \frac{1}{r^2}\right)\frac{1}{r^3}\begin{pmatrix} x_{b1}-x_{a1} \\ x_{b2}-x_{a2} \end{pmatrix}$$

$$\begin{pmatrix} a_{b1} \\ a_{b2} \end{pmatrix} = (1-v_b^2)\begin{bmatrix} 1-v_{b1}^2 & -v_{b1}v_{b2} \\ -v_{b1}v_{b2} & 1-v_{b2}^2 \end{bmatrix}\begin{pmatrix} k_{b1} \\ k_{b2} \end{pmatrix}$$

$$\begin{pmatrix} k_{b1} \\ k_{b2} \end{pmatrix} = \begin{pmatrix} P_{b1} \\ P_{b2} \end{pmatrix} = -Gm_a\left(1 + 3\left(\frac{H}{\mu}\right)^2 \frac{1}{r^2}\right)\frac{1}{r^3}\begin{pmatrix} x_{b1}-x_{a1} \\ x_{b2}-x_{a2} \end{pmatrix}$$

Acceleration components of fragment a and fragment b—expanded forms

$$\begin{pmatrix} a_{a1} \\ a_{a2} \end{pmatrix} = \left\{(1-v_a^2)^2\left(1+3\left(\frac{H}{\mu}\right)^2 \frac{1}{r_{ab}^2}\right)\frac{m_b}{r_{ab}^3}\begin{pmatrix} x_{b1}-x_{a1} \\ x_{b2}-x_{a2} \end{pmatrix}\right\}$$

$$-\left\{(1-v_a^2)((x_{b1}-x_{a1})v_{a2}-(x_{b2}-x_{a2})v_{a1})\frac{m_b}{r_{ab}^3}\begin{pmatrix} -v_{a2} \\ v_{a1} \end{pmatrix}\right\}$$

$$-\left\{((x_{b1}-x_{a1})v_{a2}-(x_{b2}-x_{a2})v_{a1})^3 3\left(\frac{m_a}{\mu}\right)2\frac{m_b}{r_{ab}^5}\begin{pmatrix} -v_{a2} \\ v_{a1} \end{pmatrix}\right\}$$

$$\begin{pmatrix} a_{b1} \\ a_{b2} \end{pmatrix} = -\left\{(1-v_b^2)^2\left(1+3\left(\frac{H}{\mu}\right)^2 \frac{1}{r_{ab}^2}\right)\frac{m_a}{r_{ab}^3}\begin{pmatrix} x_{b1}-x_{a1} \\ x_{b2}-x_{a2} \end{pmatrix}\right\}$$

$$+\left\{(1-v_a^2)((x_{b1}-x_{a1})v_{b2}-(x_{b2}-x_{a2})v_{b1})\frac{m_a}{r_{ab}^3}\begin{pmatrix} -v_{b2} \\ v_{b1} \end{pmatrix}\right\}$$

$$+\left\{((x_{b1}-x_{a1})v_{b2}-(x_{b2}-x_{a2})v_{b1})^3 3\left(\frac{m_b}{\mu}\right)^2\frac{m_a}{r_{ab}^5}\begin{pmatrix} -v_{b2} \\ v_{b1} \end{pmatrix}\right\}$$

$$H = m_a(x_{a1}v_{a2}-x_{a2}v_{a1})\beta_a + m_b(x_{b1}v_{b2}-x_{b2}v_{b1})\beta_b$$

dominates over the second two, and when v approaches 1, the first and second terms approach zero leaving the third term to dominate.

VII. THREE EMPIRICAL TESTS

SI is logically true under the assumptions of Eq. (1), the mathematical structure of spacetime, and the spacetime change equation, Eq. (12). One does not need to verify this. However, the question that requires empirical testing is the degree to which SI, together with the specific form of the fragment of energy given in Eq. (19), is capable of agreeing with reality. To validate SI, we challenged it with three empirical tests. The tests corresponded to different physical environments that one might loosely characterize as mechanical and light and as low-curvature and high-curvature. The low-curvature mechanical environment is the one to which NT already applies, and SI converges to NT in that environment, so one does not need to test that environment. This leaves us with the three before mentioned empirical tests. The first test is of the high-curvature mechanical environment. For this test, we sought to predict the anomalous precessions of Mercury and of Jupiter. Originally, scientists verified GR, in part, by predicting the precession of Mercury, too. Therefore, the goal in this test was to match our predictions with those of GR. The second and third tests are of the low-curvature and high-curvature light environments, respectively. For the second test, we sought to predict the bending of light when it grazes the sun. Again, the original verification of GR employed this test. Therefore, again, the goal was to match our predictions with those of GR. For the third test, we sought to determine the radius of the photon sphere—the critical radius outside of which a photon escapes the pull of a fragment of energy and inside which the fragment captures the photon. NT and the theory of special relativity do not predict the existence of photon spheres, only GR did. Furthermore, unlike in test 1 and in test 2, in GR one refers to the gravitational field in test 3 as "strong," corresponding to high Riemannian curvature. Also, it was natural to think of the black hole as a general relativistic phenomenon. Therefore, one would regard whether SI predicts the existence of a photon sphere to be particularly important, because it challenges that assumption. Furthermore, GR predicts that the radius of the photon sphere is equal to three-halves times the Schwarzschild radius.[4] Therefore, it was also of interest to determine whether our predictions agree with that result. Finally, note the three tests assess the physical behavior of bodies, but not some aberrations that result from observing them from afar. Furthermore, there is the possibility that one could find that some of SI's predictions differ from those obtained in GR. Additional tests, not considered in this article, will shed additional insight into SI's predictive capabilities. We leave tests such as those and others for the future.

Tables VIII and IX give the conversion constants between light units and conventional units. Beginning in this section, we switch the expressions of many of the quantities from light units to conventional units. Tables VIII and IX underline the quantities that are in conventional units. After that, we forgo distinguishing between light units and conventional units by underlining quantities. Table X repeats Table VII but now gives the governing equations in conventional units. Table XI lists the physical constants used in both problems. The constants are the same as those used in Ref. 1.

In the tests of the two-body models, the systems are planar, a body orbits the sun, and the sun orbits the body in the absence of external effects. We modeled the orbiting sun as fragment a and the other orbiting body as fragment b. In the bending of light tests, fragment b is massless (a photon). We determined all of the trajectories by numerical integration following the numerical approach adopted in Ref. 1. Toward matching the two-body problem results obtained here with the one-body results in Ref. 1, we started with the initial position r_p and the initial velocity v_p from the one-body problem and determined the corresponding initial conditions in the two-body problem. The state variables in the two-body problems are

$$x_1 = x_{a1}, \quad x_2 = x_{a2}, \quad x_3 = v_{a1}, \quad x_4 = v_{a2}, \quad x_5 = x_{b1}, \quad x_6 = x_{b2}, \quad x_7 = v_{b1}, \text{ and } x_8 = v_{b2}.$$

The initial conditions were set at the perihelion of the orbits

$$x_{10} = r_{ap}, \quad x_{20} = 0, \quad x_{30} = 0, \quad x_{40} = v_{ap}, \quad x_{50} = r_{bp}, \quad x_{60} = 0, \quad x_{70} = 0, \text{ and } x_{80} = v_{bp},$$

where

$$\begin{aligned} r_{ap} &= -\frac{\mu}{m_a} r_p, r_{pb} = \frac{\mu}{m_b} r_p \\ v_{ap} &= -\frac{\mu v_p}{\sqrt{m_a^2\left(1-\frac{v_p^2}{c^2}\right)+\frac{\mu^2 v_p^2}{c^2}}}, \\ v_{bp} &= \frac{\mu v_p}{\sqrt{m_b^2\left(1-\frac{v_p^2}{c^2}\right)+\frac{\mu^2 v_p^2}{c^2}}} \end{aligned} \quad . \tag{20}$$

TABLE VIII. Conversions of selected quantities between light units and conventional units.

Multiply from light unit to get conventional unit. Divide from conventional unit to get light unit. L is characteristic length.							
m	Lc^2/G	a	c^2/L	u	G/Lc^4	Q	1
x	L	e	1	A	1	M	Lc^2/G
t	L/c	k	$1/L$	P	$1/L$	L	Lc^3/G
v	c	h	Lc	F	c^4/G	H	L^2c^3/G

TABLE IX. Conversions of selected equations between light units and conventional units.

Light units	Conventional units
$A = mu$	$\underline{A} = m c^2 \underline{u}$
$P = \frac{\partial A}{\partial x}$	$\underline{P} = \frac{\partial \underline{A}}{\partial \underline{x}}$
$F = mP = \frac{dL}{ds}$	$\underline{F} = \underline{m} c^2 \underline{P} = c \frac{d\underline{L}}{d\underline{s}}$
$Q = (x_r - x_{0r})P_s - (x_{as} - x_{0s})P_r$	$\underline{Q} = (\underline{x}_r - \underline{x}_{0r})\underline{P}s - (\underline{x}_s - \underline{x}_{0s})\underline{P}_r$
$L_r \triangleq m e_r$	$\underline{L}_r \triangleq \underline{m} \underline{e}_r c$
$M = mQ = \frac{dH}{ds}$	$\underline{M} = \underline{m}\underline{Q} = c \frac{d\underline{H}}{d\underline{s}}$
$H_t \triangleq m h_t \ = m\big((x_r - x_{0r})e_s - (x_{as} - x_{0s})e_r\big)$	$\underline{H}_t \triangleq \underline{m} \underline{h}_t \ = \underline{m}\big((\underline{x}_r - \underline{x}_{0r})e_s - (\underline{x}_s - \underline{x}_{0s})\underline{e}_r\big)c$
$ds^2 \triangleq dt^2 - dx_1^2 - dx_2^2 - dx_3^2$	$d\underline{s}^2 \triangleq c^2 d\underline{t}^2 - d\underline{x}_1^2 - d\underline{x}_2^2 - d\underline{x}_3^2$
$e_r \triangleq v_r \beta, \ \ \beta \triangleq (1 - v^2)^{\frac{1}{2}}$	$\underline{e}_r \triangleq \frac{v_r}{c}\beta, \qquad \beta \triangleq \left(1 - \left(\frac{v_r}{c}\right)^2\right)^{-\frac{1}{2}}$
$a_r = B_{rs} P_s \ \ B_{rs} = (1 - v^2)(-v_r v_s + \delta_{rs})$	$\underline{a}_r = \underline{B}_{rs}\underline{P}_s$
	$\underline{B}_{rs} = c^2\left(1 - \left(\frac{v_r}{c}\right)^2\right)\left(-\left(\frac{v_r}{c}\right)\left(\frac{v_s}{c}\right) + \delta_{rs}\right)$
$P = k$	$\underline{P} = \underline{k}$

Table XII contains the results from test 1, test 2, and test 3.

A. Test 1: Mechanical, high-curvature

The analytically determined precession from GR is $\delta\phi = \frac{6\pi G(m_a + m_b)}{c^2 A(1-e^2)} = 5.047 \times 10^{-7}$ rad/orbit $= 43.2$ arc sec/century for Mercury[1] and 3.607×10^{-8} rad/orbit $= 0.063$ arc sec/century for Jupiter.[e)] To verify these results, we numerically integrated the two-body accelerations to obtain the pair of trajectories for a little more than one orbit. As shown in Fig. 3, the origin of the coordinates of the Mercury-sun system is located at its mass center. Initially, both Mercury and the sun were in their perihelion positions. We determined the precise locations of the next perihelion by looking for a sign change in dr_a/dt and dr_b/dt and then numerically calculated $\delta\phi_a = x_a/r_{ap}$ and $\delta\phi_b = x_b/r_{bp}$. Figure 4 shows the calculation of the precession angle of Mercury for the Mercury-sun system. The same steps were performed for the Jupiter-sun system, not shown.

Table XII presents the numerical results of test 1. Line 1 gives the precession angles for the Mercury-sun system and for the Jupiter-sun system predicted by NT when modeled as two-body systems and, from Ref. 1, in line 2 when modeled as one-body systems. As shown, NT predicts no precession in all of the cases. Line 3 gives the precession angles predicted by SI when modeled as two-body systems, and line 4 gives the precession angles predicted by GR, which is the standard against which the test assesses SI. As shown, GR models the Mercury-sun system and the Jupiter-sun system as one-body systems. One also sees that the precession angle of Mercury predicted by two-body SI agrees with the GR prediction to three decimal places. The precession angle of Jupiter predicted by two-body SI is 3.592×10^{-8} rad/orbit and by GR is 3.607×10^{-8} rad/orbit, so they differ in the second decimal. Although the error is very small, we expected to see some error due to the mass center speed limitation mentioned in Section IV, which accounts for tiny differences between the results of a two-body model and a one-body model, recalling that the GR result employs a one-body model. Lines 5–8 address this difference. Line 5 shows the precession angles for the two-body SI model without the limiting condition, and line 6 takes the difference between lines 5 and 6. Line 7 shows the precession angles for the one-body SI with the spacetime limiting condition.[1] As shown, the differences between the two-body results and the one-body SI results in line 6 and the one-body SI results in line 7 are in agreement with GR to three decimal places, essentially in full agreement with GR. Finally, as mentioned previously, the mass center speed limitation accounts for tiny differences between the results of a two-body model and a one-body model. When employing one-body models, the precession angles of the sun were equal to the precession angles of the other bodies. On the other hand, when employing two-body models, the precession angles of the sun differ slightly from the precession angles of the other bodies, as shown in lines 3 and 5.

B. Test 2: Light, low-curvature

The analytically determined sun grazing bend angle of light from GR is $\delta_N = \frac{4GM}{c^2 r_p} = 8.534 \times 10^{-6}$ rad $= 1.760$ arc sec,[1] where r_p is the distance of closest approach. To verify this result, we set the distance of closest approach to the radius R_s

[e)] David R. Williams (2020), "Jupiter Fact Sheet," NASA Goddard Space Flight Center https://nssdc.gsfc.nasa.gov/planetary/factsheet/jupiterfact.html

of the sun. We then simulated the two-body (photon-sun) responses two different ways. The first way, we set the mass of the photon to be very close to zero ($m_b = 1\times10^{-12}$) and the speed of the photon to be a very small amount less than the speed of light ($v_p = 0.9999c$). We then calculated the initial conditions from Eq. (20) and finally simulated the response of the two-body system. The second way, we set the mass of the photon equal to zero and the speed of the photon equal to the speed of light. This reduced the acceleration components of the sun to zero meaning it remained stationary. When doing this, one would obtain a divide by zero error if numerically integrating the equations governing the motion of the photon without any modification of the equations. To overcome this, one can use L'Hopital's rule or, in this case, simply cancel terms that go to zero, and obtain

$$\begin{pmatrix} a_{b1} \\ a_{b2} \end{pmatrix} = -\frac{3Gm_a}{r^5}\left(x_{b1}\frac{v_{b2}}{c} - x_{b2}\frac{v_{b1}}{c}\right)^2 \times \begin{bmatrix} 1-\left(\frac{v_{b1}}{c}\right)^2 & -\left(\frac{v_{b1}}{c}\right)\left(\frac{v_{b2}}{c}\right) \\ -\left(\frac{v_{b1}}{c}\right)\left(\frac{v_{b2}}{c}\right) & 1-\left(\frac{v_{b2}}{c}\right)^2 \end{bmatrix} \begin{pmatrix} x_{b1} \\ x_{b2} \end{pmatrix}. \tag{21}$$

We then calculated the initial conditions from Eq. (20), setting the initial positions and initial velocities of the photon and the sun to $r_a = 0, r_b = r_p = R_s, v_a = 0,$ and $v_b = c$. Figure 5 shows the trajectory of the photon released from the perihelion position on the x_1 axis. Both ways of calculating the numerical results produced the same photon trajectory and bend angle, in agreement with GR; see line 9 of Table XII.

C. Test 3: Light, high-curvature

For the third test, we examined the full path trajectory of a photon as it approaches a point gravitational source. Again, we used the mass of the sun for the source. We solved the problem two ways, first releasing the photon in the neighborhood of the photon sphere (locally) and next releasing the photon from a distance that is large compared with the radius of the photon sphere (distant location). For a photon released in the neighborhood of 1.5 times the Schwarzschild radius r_s, which is the photon sphere radius $r = 1.5r_s$, the light transitions from sun capture to photon escape. In this problem, we let: $m_a = M, m_b = 0, r_p = 1.5r_s,$ and $v_p = c$,where the Schwarzschild radius is $r_s = \frac{2GM}{c^2}$. The initial conditions are $r_a = 0, r_b = 1.5r_s, v_a = 0,$ and $v_b = c$. These initial conditions are for a stationary observer in inertial space; they correspond to the local observer in GR. For the photon released from a large distance away from the photon sphere, we set up initial conditions that are equivalent to the set up in GR, employing the impact parameter b.[4] In GR, one numerically solves the differential equation $\frac{d^2u}{d\phi^2} + u = \frac{3GM}{c^2}u^2$, where $u = 1/r$ and where r and ϕ are spherical coordinates in the equatorial plane. For the initial conditions, we set $u = \frac{1}{100r_s}$ and $\frac{du}{d\phi} = u\cdot\cot\phi$ at $\phi = \sin^{-1}bu$, where b is the impact parameter shown in Fig. 6(a). We then plotted the trajectory of the photon using the coordinates $x_1 = r\cos\phi$ and $x_2 = r\sin\phi$ [see Fig. 6(b)]. In SI, one numerically integrates in time using the accelerations given in Eq. (21). The initial conditions for the photon released at a distance are $x_{b1} = 100r_s, x_{b2} = b$ (variable), $v_{b1} = -c,$ and $v_{b2} = 0$. Note that the numerical results described below, wherein we released the photon from a distance equal to $100r_s$ yields practically identical results to those obtained by releasing the photon at infinity.

Figure 6(b) shows the full path trajectories of photons predicted by SI and GR, where b was taken as $(1.001)3\sqrt{3}\frac{r_s}{2}$, $3\sqrt{3}\frac{r_s}{2}$, and $(0.999)3\sqrt{3}\frac{r_s}{2}$. For the intermediate value of $b = 3\sqrt{3}\frac{r_s}{2}$, the predicted orbit as the photon approaches the source is circular at $r = 1.5r_s$,in agreement with the well-known GR result. As shown, we get

TABLE X. Governing equations for the two-body problems in conventional units.

Acceleration compo*nents of fragment a and fragment b

$$\begin{pmatrix} a_{a1} \\ a_{a2} \end{pmatrix} = c^2\left(1-\left(\frac{v_a}{c}\right)^2\right)\begin{bmatrix} 1-\left(\frac{v_{a1}}{c}\right)^2 & -\left(\frac{v_{a1}}{c}\right)\left(\frac{v_{a2}}{c}\right) \\ -\left(\frac{v_{a1}}{c}\right)\left(\frac{v_{a2}}{c}\right) & 1-\left(\frac{v_{a2}}{c}\right)^2 \end{bmatrix}\begin{pmatrix} k_{a1} \\ k_{a2} \end{pmatrix}$$

$$\begin{pmatrix} k_{a1} \\ k_{a2} \end{pmatrix} = \begin{pmatrix} P_{a1} \\ P_{a2} \end{pmatrix} = G\frac{m_b}{c^2}\left(1+3\left(\frac{H}{\mu c}\right)^2\frac{1}{r^2}\right)\frac{1}{r^3}\begin{pmatrix} x_{b1}-x_{a1} \\ x_{b2}-x_{a2} \end{pmatrix}$$

$$\begin{pmatrix} a_{b1} \\ a_{b2} \end{pmatrix} = c^2\left(1-\left(\frac{v_b}{c}\right)^2\right)\begin{bmatrix} 1-\left(\frac{v_{b1}}{c}\right)^2 & -\left(\frac{v_{b1}}{c}\right)\left(\frac{v_{b2}}{c}\right) \\ -\left(\frac{v_{b1}}{c}\right)\left(\frac{v_{b2}}{c}\right) & 1-\left(\frac{v_{b2}}{c}\right)^2 \end{bmatrix}\begin{pmatrix} k_{b1} \\ k_{b2} \end{pmatrix}$$

$$\begin{pmatrix} k_{b1} \\ k_{b2} \end{pmatrix} = \begin{pmatrix} P_{b1} \\ P_{b2} \end{pmatrix} = -G\frac{m_a}{c^2}\left(1+3\left(\frac{H}{\mu c}\right)^2\frac{1}{r^2}\right)\frac{1}{r^3}\begin{pmatrix} x_{b1}-x_{a1} \\ x_{b2}-x_{a2} \end{pmatrix}$$

Acceleration components of fragment a and fragment b—expanded form

$$\begin{pmatrix} a_{a1} \\ a_{a2} \end{pmatrix} = \left\{\left(1-(v_a/c)^2\right)^2\left(1+3\left(\frac{H}{\mu c}\right)^2\frac{1}{r_{ab}^2}\right)\frac{Gm_b}{r_{ab}^3}\begin{pmatrix} x_{b1}-x_{a1} \\ x_{b2}-x_{a2} \end{pmatrix}\right\}$$

$$-\left\{\left(1-(v_a/c)^2\right)((x_{b1}-x_{a1})v_{a2}-(x_{b2}-x_{a2})v_{a1})\frac{Gm_b}{c^2r_{ab}^3}\begin{pmatrix} -v_{a2} \\ v_{a1} \end{pmatrix}\right\}$$

$$-\left\{((x_{b1}-x_{a1})v_{a2}-(x_{b2}-x_{a2})v_{a1})^3\left(\frac{m_a}{\mu c}\right)^2\frac{Gm_b}{c^2r_{ab}^5}\begin{pmatrix} -v_{a2} \\ v_{a1} \end{pmatrix}\right\}$$

$$\begin{pmatrix} a_{b1} \\ a_{b2} \end{pmatrix} = \left\{\left(1-(v_b/c)^2\right)^2\left(1+3\left(\frac{H}{\mu c}\right)^2\frac{1}{r_{ab}^2}\right)\frac{Gm_a}{c^2r_{ab}^3}\begin{pmatrix} x_{b1}-x_{a1} \\ x_{b2}-x_{a2} \end{pmatrix}\right\}$$

$$+\left\{\left(1-(v_b/c)^2\right)((x_{b1}-x_{a1})v_{b2}-(x_{b2}-x_{a2})v_{b1})\frac{Gm_a}{c^2r_{ab}^3}\begin{pmatrix} -v_{b2} \\ v_{b1} \end{pmatrix}\right\}$$

$$+\left\{((x_{b1}-x_{a1})v_{b2}-(x_{b2}-x_{a2})v_{b1})^3\left(\frac{m_b}{\mu c}\right)^2\frac{Gm_a}{c^2r_{ab}^5}\begin{pmatrix} -v_{b2} \\ v_{b1} \end{pmatrix}\right\}$$

$$H = m_a(x_{a1}v_{a2}-x_{a2}v_{a1})\beta_a + m_b(x_{b1}v_{b2}-x_{b2}v_{b1})\beta_b$$

TABLE XI. Physical constants in conventional units (Ref. 1).[e)]

		Mercury	Jupiter
m	Mass	3.3022×10^{23} kg	1.898×10^{27} kg
r_p	Perihelion radius	4.60012×10^{10} m	74.05×10^{10} m
A	Semimajor axis	57.91×10^{9} m	778.57×10^{9} m
e	Eccentricity of the orbit	0.20566	0.04890
v_p	Perihelion velocity	58.98×10^{3} m/s	13.72×10^{3} m/s
T	Orbital period	87.969 Earth days = 7 600 530 s	4333 Earth days = 374 371 200 s
		Sun	
M	Mass	1.989×10^{30} kg	
R_s	Radius	696 000 000 m	
r_s	Schwarzschild radius	2970 m	
		Other	
G	Gravitational constant	6.674×10^{-11} $m^3/kg\ s^2$	
c	Speed of light	2.99×10^{8} m/s	

TABLE XII. Numerical results of test 1, test 2, and test 3.

		Precession angles of Mercury and Jupiter (rad/orbit)			
	Test 1	Mercury	Sun	Jupiter	Sun
1	Two-body NT	$<10^{-13}$	$<10^{-13}$	$<10^{-13}$	$<10^{-13}$
2	One-body NT (Ref. 1)	$<10^{-13}$	$<10^{-13}$	$<10^{-13}$	$<10^{-13}$
3	Two-body SI with adjustment	5.047×10^{-7}	1.200×10^{-7}	3.593×10^{-8}	1.742×10^{-7}
4	**GR**	$\mathbf{5.047 \times 10^{-7}}$	**—**	$\mathbf{3.607 \times 10^{-8}}$	—
5	Two-body SI no limiting condition	$<10^{-13}$	6.967×10^{-7}	-1.320×10^{-10}	1.382×10^{-7}
6	Two-body SI difference	5.047×10^{-7}	5.033×10^{-7}	3.606×10^{-8}	3.600×10^{-8}
7	One-body SI with limiting condition (Ref. 1)	5.047×10^{-7}	—	3.606×10^{-8}	—
8	Error	**0.000%**		**-0.028%**	
	Test 2	**Light grazing bend angle** (rad)			
9	SI	8.534×10^{-6}	GR	8.534×10^{-6}	Error **0%**
	Test 3	**Photon sphere radius** ($r_s = 2GM/c^2$)			
10	SI	$1.500\ r_s$	GR	$1.500\ r_s$	Error **0%**

a stable orbit when slightly decreasing the impact parameter from $3\sqrt{3}\frac{r_s}{2}$, during which the source captures the photon, and we get an unstable orbit when slightly increasing the impact parameter from $3\sqrt{3}\frac{r_s}{2}$. In this instance, after orbiting the source once, the photon trajectory approaches asymptotically a straight path, never to return to the source.

This test confirms that SI predicts the existence of the photon sphere. Also, the photon sphere's radius is in agreement with GR for the static isotropic case, which corresponds to the Schwarzschild metric. Additionally, as shown in Fig. 6(b), the spatial paths predicted by SI and the spatial paths predicted by GR are the same (overlap). Indeed, although not shown, the spatial paths in SI and in GR were the same for the precession of Mercury problem in Fig. 4 and the bending of light problem in Fig. 5, too. For completeness, line 10 of Table XII records the agreement of this photon sphere result with GR.

One can also derive analytically from SI the radius of the photon sphere. From Table X, the GR result is $r = 1.5r_s = 3GM/c^2$. From Table VII, imposing a circular motion of constant radius r and of constant speed c, $\begin{pmatrix} a_{b1} \\ a_{b2} \end{pmatrix} = -3\frac{GM}{r^3}\begin{pmatrix} x_{b1} \\ x_{b2} \end{pmatrix}$. We also know for circular motion that the components of acceleration are $\begin{pmatrix} a_{b1} \\ a_{b2} \end{pmatrix} = -\frac{c^2}{r^2}\begin{pmatrix} x_{b1} \\ x_{b2} \end{pmatrix}$. Equating the components of acceleration, we get $r = 3GM/c^2$, in agreement with the SI numerical results and with GR.

VIII. HISTORICAL CONTEXT AND CONCEPTUAL IMPLICATIONS

The purpose of the empirical results was to validate that SI is in agreement with the well-known results for the case of a static isotropic source. This section places the development of SI in historical context and briefly discusses conceptual implications.

The principle of impetus dates back to antiquity. Historians believe that ancient impetus began with Aristotle (384–322 BC) and continued with such figures as Philoponus (490–570), Avicenna (980–1037), Abu'l-Barakat (c.1080–c.1164), Nur ad-Din al-Bitruji (died c. 1204), Jean Buridan (c.1301–s.1359), and Galileo (1564–1642). Classical impetus arose in 1687 in *Mathematical Principles of Natural Philosophy* by Sir Isaac Newton (1643–1727). The concept of impetus that we adopted here, consistent with FT, expressed it in terms of fragments of energy, fields, and spacetime.

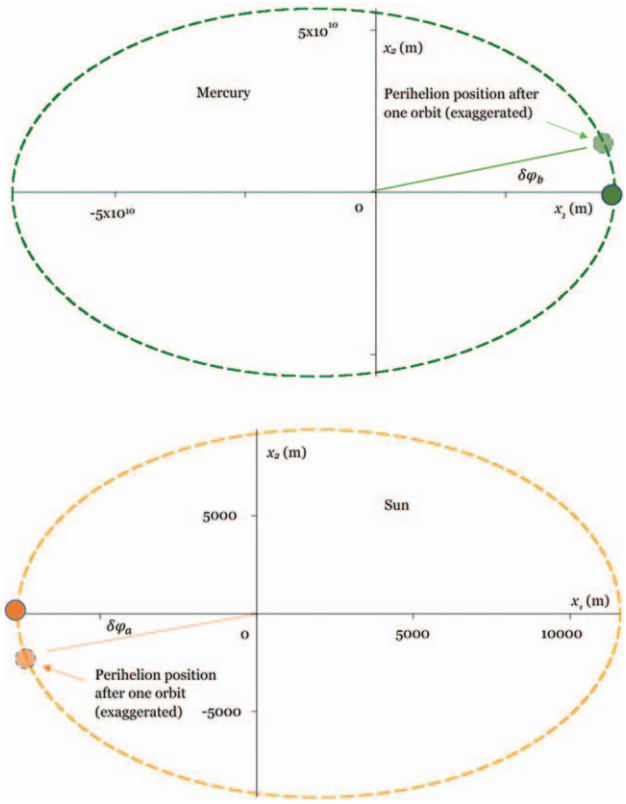

FIG. 3. Trajectories of Mercury and the sun.

Conceptually, this article gives perhaps two principal results. The first is that SI extends NT, previously applicable to particle problems, to problems involving both mechanical particles and light waves, and it does so in a single formulation that stands on its own. Of course, GR was the first theory to accomplish this, but this theory did it differently. Instead of replacing mass and force with curved spacetime, SI "modernized" the concept of impetus, uniting NT and GR. The second contribution pertains to the resolution that SI brings to conceptual questions that were paradoxical in (unanswered by) NT, which has importance in that it contributes to our understanding of the unification of the continuum theories (NT, EM, GR, and FT).

Pertaining to the extension of NT, we know that NT never explicitly addressed light phenomena, which EM addressed directly. Furthermore, historically, scientists adopted spacetime in FT to address the electromagnetic

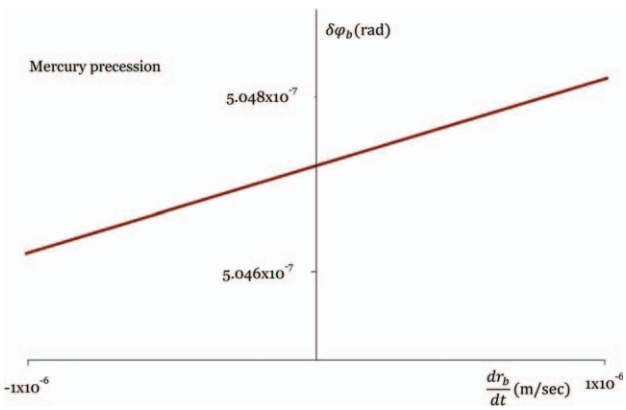

FIG. 4. Mercury precession angle.

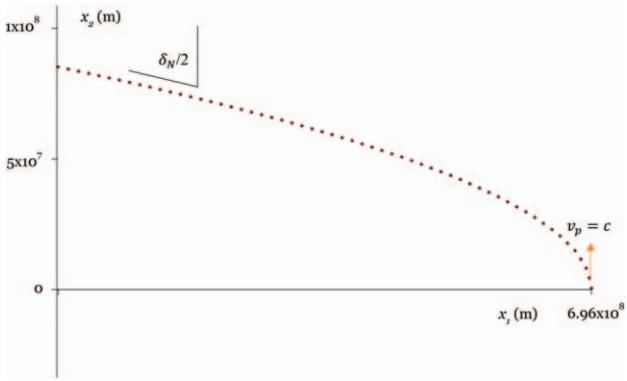

FIG. 5. Bend angle of photon grazing the sun.

behavior found in EM. Therefore, one should find it natural in the modernization of the concept of impetus that we replaced ordinary geometry in NT with spacetime geometry and that we transitioned from the particle concept to the field concept. Again, the key was to replace the classical primitives—the particle and the wave—with a single primitive—the fragment of energy—to accommodate both particle and wave processes. As Section II showed, two fragments of energy, merely by their radial dependence, exhibit relationships that one already finds in NT, making the connection of the concept of impetus from NT to FT somewhat anticipated.

Pertaining to the resolutions that SI brings to longstanding paradoxes in NT, let us first consider the primitive, next, the confusion with mass, and finally the confusion with force.

First, about the primitive, NT employed the concept of the particle. The particle represented a spatial point together with one or more properties (mass in NT plus charge in EM). According to this view, the universe is a constellation of particles separated by a void (absence of particles). This view led to long-standing questions about the mechanism by which particles interact, given that the void conceptually implies isolation. EM moved toward resolving this paradox by employing the field concept but it did not completely resolve the paradox, because it continued to employ the particle from NT. There was still a need for universality in the restricted sense of concepts that cut across the continuum theories (NT, EM, GR, and FT). In this sense, the concepts of space, time, and energy were already universal but the primitives were not. EM was still employing the particle primitive that originated with NT, and its electromagnetic wave primitive lacked a source term. The development of the fragment of energy primitive unites NT and EM, completing the unification of space, time, and energy. In the new view, the universe is a constellation of fragments of energy. There is no void, and the overlap between fragments allows one fragment to experience a change from another. The elimination of the void and its replacement with an experience of change resolves the paradox of the particle primitive in NT and the electromagnetic wave primitive in EM.

Next, about the confusion with mass, NT set two masses—inertial mass and gravitational mass—equal to each other without a logical explanation. The two seemed to exhibit seemingly contradictory behaviors. Inertial mass

seemingly impeded acceleration (hence the word "inertial") and gravitational mass resulted in bodies accelerating toward the earth independent of mass. The paradox arose in the unanswered question as to why the two masses are equal. Historically, it motivated the equivalence principle, and subsequently GR served as one remedy to the paradox. SI resolves this paradox in a simpler way. SI interprets mass as fundamentally the intensity of a fragment of energy. In SI, one describes the concept of impetus of, say, fragment a by the change equation $P_{ar} = k_{ar}$ in which k_{ar} are the path curvature components of fragment a and P_{ar} are the action force components by fragment b (in the two-body problem) that fragment a experiences. Notice that the change equations for fragment a depend on the mass of fragment b and *not* on the mass of fragment a, because P_{ar} is from fragment b. Recall that we *deduced* the interaction force acting on fragment a from the definition of the action force acting on fragment a ($F_{ar} = m_a P_{ar}$), where m_a is the mass *on which* the force acts. If we multiply the change equation $P_{ar} = k_{ar}$ by the mass m_a, we get $F_{ar} = m_a k_{ar}$. Finally, consider that $k_{ar} \cong a_{ar}$ (in light units) when the motion is slow compared with the speed of light. This yields Newton's second law (law of inertia) $F_{ar} = m_a a_{ar}$. Both the gravitational mass and the inertial mass originate from the intensity of a fragment.

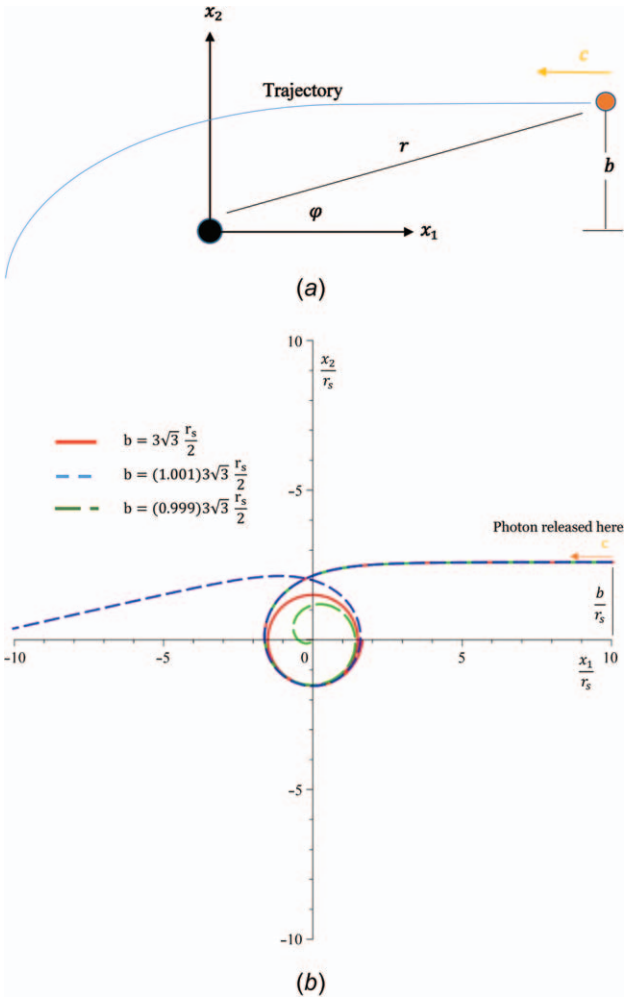

FIG. 6. (a) Setup of photon trajectory problems for GR and SI. (b) Photon trajectories reaching the neighborhood of the photon sphere for SI and GR.

One now sees too that Newton's second law—the law of inertia—creates the illusion that the acceleration components a_{ar} of body a are *inversely* proportional to its mass, serving to impede a change in velocity, when in fact, by the change equations, more fundamentally the acceleration components of body a are *linearly* proportional to the mass of body b. The present-day classical form of the second law is a slight-of-hand in mass. Furthermore, strictly speaking, the law in NT has the appearance of violating the principle of impetus, which requires that the change of the state of a primitive *not* depend on itself. In any event, we now deduce that the mass in the law of inertia and the mass in the gravitational law both originate from the mass of their fragment, which resolves the paradox of inertial and gravitational masses.

About the confusion with force, the new theory resolves the paradox in NT that originated from never clarifying whether the force F in $F = ma$ is an interaction force or an action force (NT never successfully distinguished between the two). When one thought of it as an action force, the equality of the magnitudes of mutual forces became paradoxical. For example, NT predicts that the magnitude of the force F by the comparatively huge sun on the earth is equal to the magnitude of the force F by the comparatively tiny earth back on the sun, which would be counter-intuitive if one were to think of the force as an action by a primitive. In contrast, the magnitude of the action force by the sun on the earth and the magnitude of the action force by sun back on the earth that SI predict are proportional to their respective masses, in agreement with intuition, and we now can regard the equal and opposite properties associated with interactions to be deduced, not assumed.

IX. SUMMARY

This article introduced the theory of SI. The theory unites NT and the theory of GR. It does so by replacing the law $F = ma$ governing the motion of particles with the change equation $P = k$ governing the motion of fragments of energy, where F is an interaction force, P is an action force, m is mass, a is acceleration, and k is the path curvature of the spacetime path of a source point of a fragment.

In this article, the reader discovers that the fragment of energy building block, first introduced in Ref. 1, was not a mere coincidence but rather the basis for the extension of the concept of impetus to bodies that travel at the speed of light, in general agreement with the theory of GR. To illustrate just how SI extends the concept of impetus, let us consider a simple illustration—the pair of companion problems of the Earth orbiting the sun and of light bending around the sun. In both problems, the sun pulls on a body that would otherwise travel along a straight line, causing it to rotate (orbit or bend). In classical thinking, one treats the sun as a particle of mass M, the Earth as a particle of mass m, and light as a wave, and we now treat each of them as fragments of energy. In SI, the Earth and light fragments change their directions of travel due to the gravitational force by the sun fragment. In Section II, we found the fragment of energy to lead naturally to a new mathematical structure within the FT framework that connects rigorously to one another such concepts

as mass, energy, action, and interaction. In particular, the interaction force was derived from the action force; the interaction force acting on the earth fragment or the light fragment by the sun fragment was equal to the action force by the sun fragment multiplied by the mass of the fragment on which it acts (the earth or light), written $F = mP$. Substituting this expression into the spacetime change equation $P = k$ gave $F = mk$, which *almost* looked like Newton's classical law of inertia $F = ma$ governing the motion of a particle. The difference between SI and the classical concept of impetus was in the path curvature k of a path in spacetime replacing the acceleration a of a path in space. Here, it is good to recall from Section III that $a = k$ (in light units) when the speed of a fragment is small compared with the speed of light, corresponding to the range of speeds over which the classical concept of impetus applied. The path curvature k served to predict the change that occurs when the speed of the fragment approaches that of light, too. To see how this enabled the correct prediction, let us continue with the pair of companion problems, and first recognize, regardless of whether the fragment represents the earth or light, that the sun's gravitational force acts along the line between it and the sun fragment (recall Fig. 2). Furthermore, the specific fragment derived in Section VI prevented the effect of the sun's gravitational force from vanishing when the speed of the fragment on which it acts approaches that of light. When the speed of a fragment is small when compared with the speed of light, the fragment's acceleration is along the line between the two fragments, as in NT. However, when the speed of a fragment approaches the speed of light, its acceleration vector due to the gravitational force acting on it rotates. Its acceleration vector approaches a direction that is perpendicular to its velocity vector (see Fig. 2). The absence of a component of acceleration tangent to a fragment's velocity vector creates a limit to the speed of a fragment and the nonvanishing perpendicular component of acceleration causes its path to bend. As Section III describes, light obeys the identical limiting conditions that the motion of the source of any fragment obeys.

To verify SI, we conducted three tests. Test 1 was a high-curvature mechanical test that predicted the precessions of Mercury and of Jupiter, test 2 was a low-curvature light test that predicted the bending of light when it grazes the sun, and test 3 was a high-curvature light test that predicted the photon sphere's radius. Test 3 is particularly noteworthy, because it showed that one no longer needs to regard the black hole as a general relativistic phenomenon—resulting from the bending of spacetime.

Finally, note that we expressed the equations of motion in terms of Cartesian coordinates and time, and they are relatively simple to solve. Undergraduate students in science and engineering and others with similar mathematical skills can validate the results for themselves.

APPENDIX A: SPACETIME OPERATIONS

Let x_r $(r = 0, 1, 2,$ and $3)$ denote spacetime coordinates. We designate x_0 to be a time coordinate t and the other three to be spatial coordinates. The square of a spacetime metric is

$$ds^2 \triangleq dt^2 - dx_1^2 - dx_2^2 - dx_3^2 .$$

Letting $w_{st} = w_{ts} = \begin{bmatrix} 1 & 0 & 0 & 0 \\ 0 & -1 & 0 & 0 \\ 0 & 0 & -1 & 0 \\ 0 & 0 & 0 & -1 \end{bmatrix}$, we rewrite the square of the spacetime metric as

$$ds^2 \triangleq w_{st} x_s x_t. \tag{A1}$$

In Eq. (A1), we sum repeated indices from 0 to 3. The spacetime metric motivates operations on first-order tensors that determine components and generalized perpendiculars. Table XIII gives the spacetime scalar product of two first-order tensors, the spacetime magnitude of a first-order tensor, and the generalized perpendiculars to the first-order tensors for 2D, 3D, and 4D spacetimes.

In Table XIII, the 2D, 3D, and 4D permutation symbols $\varepsilon_{rs}, \varepsilon_{rst},$ and ε_{rstu} are equal to 0 when any one index is repeated, and they are equal to 1 when their indices are in the right-hand order, and equal to -1 when in the left-hand order. Switching a pair of adjacent indices causes the sign of a permutation symbol to change. By convention, $\varepsilon_{01} = 1$ for 2D, $\varepsilon_{012} = 1$ for 3D, and $\varepsilon_{0123} = 1$ for 4D. In Table XIII, $a \cdot b = 0$ for the 2D perpendicular, $a \cdot c = b \cdot c = 0$ for the 3D perpendicular, and $a \cdot d = b \cdot d = c \cdot d = 0$ for the 4D perpendicular. The operations given in Table XIII are natural extensions to the operations that one finds with the ordinary metric in ordinary geometry for 2D, 3D, and 4D spaces.

TABLE XIII. Spacetime operations.

Dot product	$a \cdot b = a'_r b_r$	$a'_r = w_{rs} a_s$
Magnitude	$\lvert a \rvert = \sqrt{a \cdot b}$	
2D perpendicular	$b_r = \varepsilon_{rs} a'_s$	ε_{rs} $(r, s = 0, 1)$
3D perpendicular	$c_r = \varepsilon_{rst} a'_s b'_t$	ε_{rst} $(r, s, t = 0, 1, 2)$
4D perpendicular	$d_r = \varepsilon_{rstu} a'_s b'_t c'_u$	ε_{rstu} $(r, s, t, u = 0, 1, 2, 3)$

APPENDIX B: LINEAR MOMENTUM AND ANGULAR MOMENTUM INVARIANTS FOR N-BODY SYSTEMS

Consider a system of n fragments

$$A_a \triangleq m_a u(r_a), (a = 1, 2, \ldots, n), \tag{B1}$$

where m_a is the mass, $r_a^2 = (x_1 - x_{a1})^2 + (x_2 - x_{a2})^2 + (x_3 - x_{a3})^2$ is the square of the distance between a point in space and the source point of a fragment, and $u(r_a)$ is a unit fragment. (Note whereas a and b will refer here to running indices, that in the body of the article a and b were designations for particular fragments.) The following identities hold for any indices a and b between 1 and n

$$\begin{aligned} r_a|_b = r_b|_a \triangleq r_{ab}, \frac{\partial r_a}{\partial x_s} &= \frac{x_s - x_{as}}{r_a} = -\frac{\partial r_a}{\partial x_{as}}, \frac{\partial r_b}{\partial x_s}|_a \\ &= -\frac{\partial r_a}{\partial x_s}|_b \quad u(r_a)|_b = u(r_b)|_a, \frac{du(r_a)}{dr_a}|_b \\ &= \frac{du(r_b)}{dr_b}|_a \quad \frac{\partial A_a}{\partial x_s} = m_a \frac{du(r_a)}{dr_a}\frac{\partial r_a}{\partial x_s} = -\frac{\partial A_a}{\partial x_{as}}. \end{aligned} \tag{B2}$$

Let us first define the s-th component of the action force on fragment a by fragment b as

$$P_{abs} \triangleq \frac{\partial A_b}{\partial x_s}|_a = G_{ab}(x_{bs} - x_{as}), G_{ab} \triangleq \frac{du(r_b)}{dr_b}|_a \frac{m_b}{r_{ab}}. \quad \text{(B3)}$$

It follows from Eqs. (B2) and (B3) that:

$$m_a G_{ab} + m_b G_{ba} = 0, m_a P_{abs} + m_b P_{bas} = 0. \quad \text{(B4)}$$

Based on the action forces, define the interaction forces between fragments a and b and obtain from Eq. (B4) the equal and opposite properties of pairs of interaction forces

$$F_{abs} \triangleq m_a P_{bas}, F_{abs} + F_{bas} = 0. \quad \text{(B5)}$$

Next, turn to the moment components. Define the t-th component of the action moment on fragment a by fragment b and obtain from Eq. (B5), the properties of action moment pairs

$$\begin{aligned} Q_{abt} \triangleq (x_{ar} - x_{0r})P_{abs} - (x_{as} - x_{0s})P_{abr}, m_a Q_{abt} \\ + m_b Q_{bat} = 0, \end{aligned} \quad \text{(B6)}$$

where (r, s, t) is a right-handed triad. Based on the action moments, define the interaction moments between fragments a and b and obtain from Eqs. (B5) and (B7) the equal and opposite properties of pairs of interaction moments

$$M_{abt} \triangleq m_a Q_{abt}, M_{abt} + M_{bat} = 0. \quad \text{(B7)}$$

These definitions and properties provide the set up for examining the invariance of system linear momentum and of system angular momentum. The linear momentum of a fragment, the linear momentum of the system, the angular rate of a fragment, the angular momentum of a fragment, and the angular momentum of the system are

$$\begin{aligned} &L_{ar} \triangleq m_a e_{ar}, L_r \triangleq \sum_{a=1}^{n} L_{ar} \\ &h_{at} \triangleq (x_{ar} - x_{0r})e_{as} - (x_{as} - x_{0s})e_{ar}, \\ &H_{at} \triangleq m_a h_{at}, H_t \triangleq \sum_{a=1}^{n} H_{at}. \end{aligned} \quad \text{(B8)}$$

The spacetime change equations for a system of n fragments and the resultant action forces are

$$P_{as} = k_{as}, P_{as} \triangleq \sum_{b \neq a}^{n} P_{abs}, (s = 1, 2, 3). \quad \text{(B9)}$$

Thus, from Eqs. (B8) and (B9), the change in system linear momentum and the change in system angular momentum are calculated

$$\begin{aligned} \frac{dL_r}{ds} &\triangleq \sum_{a=1}^{n} \frac{dL_{ar}}{ds_a} = \sum_{a=1}^{n} m_a k_{ar} = \sum_{a=1}^{n} m_a P_{ar} = 0 \\ \frac{dH_t}{ds} &\triangleq \sum_{a=1}^{n} \frac{dH_{at}}{ds_a} \\ &= \sum_{a=1}^{n} m_a \left((x_{ar} - x_{0r})k_{as} - (x_{as} - x_{0s})k_{ar} \right) \\ &= \sum_{a=1}^{n} m_a \left((x_{ar} - x_{0r})P_{as} - (x_{as} - x_{0s})P_{ar} \right) = 0. \end{aligned} \quad \text{(B10)}$$

Thus, system linear momentum and system angular momentum are invariant.

[1]L. M. Silverberg and J. W. Eischen, Phys. Essays **33**, 489 (2020).
[2]L. M. Silverberg, *Unified Field Theory* (Wiley-VCH, Hoboken, NJ, 2009).
[3]A. A. Ungar, *Beyond the Einstein Addition Law and Its Gyroscopic Thomas Precession* (Kluwer, Dordrecht, The Netherlands, 2001).
[4]M. P. Hobson, G. Efstathiou, and A. N. Lasenby, *General Relativity* (Cambridge University Press, Cambridge, UK, 2005).